Articles

Multiple Isomerism (*cis/trans*; *syn/anti*) in $[(dmso)_2Pt(aryl)_2]$ Complexes: A Combined Structural, Spectroscopic, and Theoretical Investigation

Axel Klein,*[,†,‡] Thilo Schurr,[†] Axel Knödler,[†] Dietrich Gudat,[†] Karl-Wilhelm Klinkhammer,[†,§] Vimal K. Jain,[∥] Stanislav Záliš,[#] and Wolfgang Kaim*[,†]

Institut für Anorganische Chemie, Universität Stuttgart, Pfaffenwaldring 55, D-70569 Stuttgart, Germany, Novel Materials and Structural Chemistry Division, Bhabha Atomic Research Centre, Mumbai 400 085, India, and J. Heyrovský Institute of Physical Chemistry, Academy of Sciences of the Czech Republic, Dolejškova 3, CZ-18 000 Prague 8, Czech Republic

Received February 2, 2005

The occurrence of *cis* or *trans* configurations in square planar diarylbis(dimethyl sulfoxide)-platinum(II) complexes with S-bonded dmso ligands and aryl = 2,3,4,5,6-pentamethylphenyl, 2,4,6-trimethylphenyl, 2,6-dimethylphenyl, 2-, 3-, and 4-methylphenyl, and phenyl has been investigated by multinuclear (^{1}H, ^{13}C, and ^{195}Pt) NMR spectroscopy and crystal structure analysis. Both methods confirm the *cis* configuration for complexes with the smaller phenyl and methylphenyl (tolyl) ligands and the *trans* configuration for the compounds with the bulkier ligands, starting from 2,6-dimethylphenyl. Spectroscopic criteria could thus be established to identify configurational isomers. For the 2-tolyl complex an additional kind of isomerism arises from the relative orientation of the two methyl substituents on the same side (*syn*) or on different sides of the coordination plane (*anti*). 2D-NMR spectroscopy allowed us to identify the conformers and to study isomerization mechanisms. DFT calculation results agree well with the experimental structures and with the spectroscopic data.

Introduction

Ever since the ingenious use of mesitylplatinum(II) complexes for mechanistic studies[1] the use of such axially protecting aryl ligands has featured prominently in platinum(II) chemistry. One particular application of this approach has also involved the stabilization of mononuclear platinum(III) species[2,3] and $Pt^{II}Pt^{III}$ mixed-valent intermediates.[4] Due to the established usage of dmso complexes as precursors for ligand substitution reactions,[5] we have employed[2,6] the $[(dmso)_2PtMes_2]$ complex as reported by Eaborn et al. (Mes = mesityl).[7] These researchers have assigned a *cis* configuration to the complex on the basis of ^{1}H NMR results, an assertion that remained initially unquestioned because this compound reacts, for example, with α-diimines such as 2,2′-bypyridine (bpy) to form products with *cis*-positioned mesityl groups. Furthermore, the reported crystal structure analysis of the related $[(dmso)_2PtPh_2]$ complex showed a *cis* configuration,[8] seemingly confirming this arrangement.

In this work we can present a correction of the earlier *cis* assignment for $[(dmso)_2PtMes_2]$ by establishing a *trans* configuration through X-ray crystallography not only for that species but also for $[(dmso)_2PtXyl_2]$, Xyl = 2,6-dimethylphenyl. For the singly methyl-substituted derivative $[(dmso)_2Pt(2\text{-}Tol)_2]$, 2-Tol = 2-methylphenyl, a *cis* configuration was found in analogy with the diphenyl compound. The introduction of two *ortho* methyl groups is obviously necessary to cause a prefer-

† Universität Stuttgart.
‡ Present address: Institut für Anorganische Chemie, Universität zu Köln, Greinstrasse 6, D-50939 Köln, Germany. E-mail: axel.klein@uni-koeln.de.
§ Present address: Johannes-Gutenberg-Universität Mainz, Institut für Anorganische Chemie, Duesbergweg 10-14, D-55099 Mainz, Germany.
∥ Bhabha Atomic Research Centre.
J. Heyrovský Institute of Physical Chemistry.

(1) (a) Basolo, F.; Pearson, R. G. *Mechanism of Inorganic Reactions*; John Wiley & Sons: New York, 1967. (b) Faraone, G.; Ricevuto, V.; Romeo, R.; Trozzi, M. *Inorg. Chem.* **1969**, *8*, 2207−2211.
(2) (a) Klein, A.; Hausen, H.-D.; Kaim, W. *J. Organomet. Chem.* **1992**, *440*, 207−217. (b) Kaim, W.; Klein, A. *Organometallics* **1995**, *14*, 1176−1186.
(3) Rieger, A. L.; Carpenter, G. B.; Rieger, P. H. *Organometallics* **1993**, *12*, 842−849.
(4) (a) Klein, A.; Hasenzahl, S.; Kaim, W.; Fiedler, J. *Organometallics* **1998**, *17*, 3532−3538. (b) Klein, A.; Kaim, W.; Hornung, F. M.; Fiedler, J.; Záliš, S. *Inorg. Chim. Acta* **1997**, *264*, 269−278.
(5) Lanza, S.; Minniti, D.; Moore, P.; Sachinidis, J.; Romeo, R. *Inorg. Chem.* **1984**, *23*, 4428−4433.
(6) (a) Klein, A.; McInnes, E. J.; Kaim, W. *J. Chem. Soc., Dalton Trans.* **2002**, 2371−2378. (b) Klein, A.; van Slageren, J.; Záliš, S. *Inorg. Chem.* **2002**, *41*, 5216−5225.
(7) Eaborn, C.; Kundu, K.; Pidcock, A. *J. Chem. Soc., Dalton Trans.* **1981**, 933−938.
(8) Bardi, R.; Del Pra, A.; Piazzesi, A. M.; Trozzi, M. *Cryst. Struct. Commun.* **1981**, *20*, 301−311.

10.1021/om050076+ CCC: $30.25
Publication on Web 07/15/2005

Table 1. Crystallographic and Structure Refinement Data of Complexes [(dmso)$_2$Pt(Ar)$_2$]^a

	Ar =			
	2-Tol (*cis,syn*)^b	2-Tol (*cis,anti*)	Xyl (*trans*)	Mes (*trans*)
formula	$C_{18}H_{26}O_2S_2Pt$	$C_{18}H_{26}O_2S_2Pt$	$C_{20}H_{30}O_2S_2Pt$	$C_{22}H_{34}O_2S_2Pt$
weight (g mol^{-1})	533.60	533.60	561.61	589.70
cryst syst	orthorhombic	monoclinic	monoclinic	monoclinic
space group	*Pbca*	$P2_1/c$	$P2_1/n$	$P2_1/c$
temperature (K)	293(2)	173(2)	173(2)	293(2)
cell *a* (Å)	9.0545(1)	13.3079(15)	9.1368(18)	7.8500(16)
b (Å)	15.0141(2)	15.8153(18)	9.3840(19)	9.2620(19)
c (Å)	29.1285(3)	18.952(2)	12.224(2)	16.002(3)
α (deg)	90	90	90	90
β (deg)	90	91.057(9)	97.83(3)	95.66(3)
γ (deg)	90	90	90	90
V (Å^3)/*Z*	3959.88(8)/8	3988.2(8)/8	1038.3(4)/2	1157.8(4)/2
ρ_{calc} (g cm^{-3})	1.790	1.777	1.797	1.692
μ (mm^{-1})/*F*(000)	7.304/2080	7.252/2080	6.969/552	6.254/584
limiting indices	$-11 < h < 11$, $-17 < k < 19$, $-37 < l < 25$	$0 < h < 16$, $0 < k < 20$, $-24 < l < 24$	$-12 < h < 12$, $0 < k < 13$, $0 < l < 17$	$-11 < h < 10$, $-12 < k < 13$, $-22 < l < 22$
no. of reflns collect./unique	39 362/4509	7978/7605	3022/3022	26 136/3357
R_{int}	0.0699	0.0512	0.0540	0.0636
no. of data/restrnts/params	4509/0/215	7605/0/413	3022/0/116	3357/1/130
GOF on F^2	1.447	0.999	1.083	3.072
final R_1, wR_2 indices [$I > 2\sigma(I)$]	$R_1 = 0.0544$, $wR_2 = 0.0991$	$R_1 = 0.0533$, $wR_2 = 0.0948$	$R_1 = 0.0424$, $wR_2 = 0.1145$	$R_1 = 0.0707$, $wR_2 = 0.1367$
R_1, wR_2 (all data)	$R_1 = 0.0745$, $wR_2 = 0.1212$	$R_1 = 0.1122$, $wR_2 = 0.1132$	$R_1 = 0.0534$, $wR_2 = 0.1233$	$R_1 = 0.0772$, $wR_2 = 0.1374$
largest diff peak and hole (e Å^{-3})	2.140 and −1.304	1.268 and −1.036	4.103 and −2.718	3.401 and −1.921

^{a} Radiation wavelength $\lambda = 0.71073$ Å. Refinement method: full-matrix least-squares on F^2. Absorption correction: empirical, psi-scans. ^{b} Absorption correction: numerical.

Table 2. Selected Bond Distances (Å) and Bond Angles (deg) of Complexes [(dmso)$_2$Pt(Ar)$_2$]

	Ar =					
	Ph (*cis*)[8]	2-Tol (*cis,syn*)	2-Tol (1) (*cis,anti*)	2-Tol (2) (*cis,anti*)	Xyl (*trans*)	Mes (*trans*)
			Distances			
Pt−S(1)	2.324(2)	2.330(2)	2.330(3)	2.324(3)	2.255(1)	2.251(2)
Pt−S(2)	2.315(2)	2.320(2)	2.328(3)	2.321(3)	2.255(1)	2.251(2)
Pt−C(1)	2.049(6)	2.022(7)	2.044(11)	2.033(8)	2.099(5)	2.111(6)
Pt−C(11)	2.043(5)	2.051(7)	2.030(10)	2.043(10)	2.099(5)	2.111(6)
Pt−C(7)		3.423(8)	3.319(11)	3.271(11)	3.298(6)	3.366(7)
Pt−C(17)/C(8)		3.329(8)	3.415(11)	3.233(12)	3.330(6)	3.295(6)
S(1)−O(1)	1.480(6)	1.481(4)	1.476(9)	1.485(11)	1.470(4)	1.466(5)
S(2)−O(2)	1.474(6)	1.484(5)	1.474(8)	1.488(8)		
			Angles			
S−Pt−S	88.9(1)	90.36(6)	92.39(10)	89.18(11)	180.00(8)	180.0(1)
C−Pt−C	87.0(2)	86.8(3)	84.9(4)	88.8(4)	180.0(2)	180.0(4)
C(1)−Pt−S(1)	92.2(2)	90.3(2)	92.3(3)	91.1(2)	90.76(13)	91.39(18)
C(1)−Pt−S(2)	176.9(2)	176.3(2)	175.3(3)	178.0(3)	89.24(13)	88.61(18)
C(11)−Pt−S(2)	92.3(2)	92.20(2)	90.5(3)	91.1(3)	90.76(13)	91.39(18)
C(11)−Pt−S(1)	173.1(1)	173.0(2)	175.4(4)	174.4(3)	89.76(13)	88.61(18)
∑ of angles	360.40	359.66	360.09	360.18	360.00	360.00
tilt CCPt/SSPt	7.6	7.3	3.7	6.0	0	0
tilt CCPtSS/aryl	86.5, 69.8	83.3, 86.0	82.3, 89.7	84.5, 89.8	80.6	83.7

ence for the *trans* arrangement as the low-energy configuration. In addition, the bis(2-tolyl) complex was observed to exist in two conformational isomers, with *syn*- and *anti*-positioned *o*-methyl groups relative to the PtC_2S_2 plane (S-bonded dmso). A detailed NMR study on a more extended series of bisarylplatinum complexes with dmso ligands, [(dmso)$_2$Pt(aryl)$_2$] (aryl = 2,3,4,5,6-pentamethylphenyl, 2,4,6-trimethylphenyl, 2,6-dimethylphenyl, 2-, 3-, and 4-methylphenyl, and phenyl) confirms the occurrence of such isomers in fluid solution.

Results and Discussion

Preparation. The complexes were prepared from the precursor complex [(dmso)$_2$PtCl$_2$] by metathesis reactions using stannanes (aryl)SnMe$_3$. As expected, the formation of the complex with the sterically demanding pentamethylphenyl ligand required the longest reaction time and highest temperature (see Experimental Section). In all cases but [(dmso)$_2$Pt(2-Tol)$_2$] we observed the formation of only one isomer, as concluded from ^{1}H NMR spectroscopy of the crude reaction products (prior to recrystallization).

Crystal Structures. The crystal and molecular structures of [(dmso)$_2$Pt(2-Tol)$_2$] (two isomers), [(dmso)$_2$Pt-(2,6-Xyl)$_2$], and [(dmso)$_2$Pt(Mes)$_2$] were determined from single-crystal XRD experiments. The compounds crystallize in monoclinic space groups ($P2_1/c$ or $P2_1/n$) with the exception of *cis,syn*-[(dmso)$_2$Pt(2-Tol)$_2$], which was solved in the orthorhombic space group *Pbca*. The results of the structure determinations are summarized in Tables 1 and 2.

For *cis,anti*-[(dmso)$_2$Pt(2-Tol)$_2$] two independent molecules are found in the unit cell. For both molecules

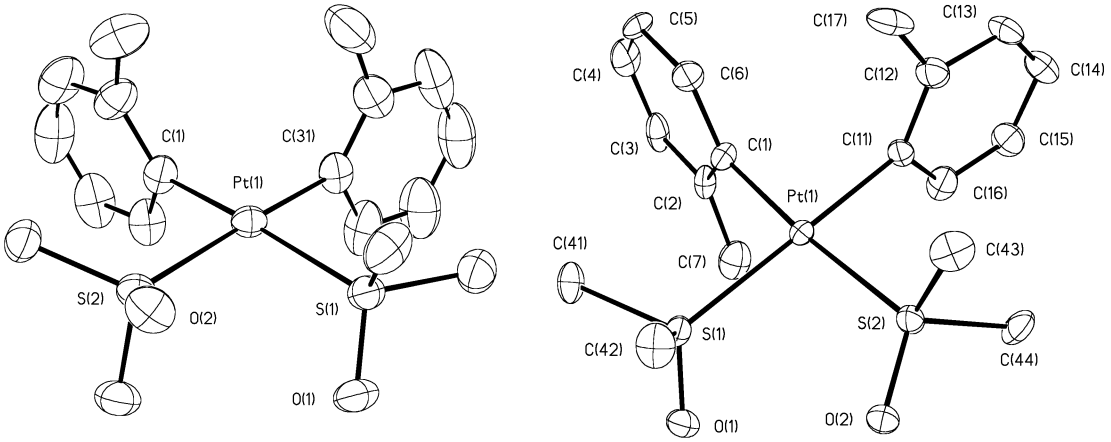

Figure 1. Molecular structures of the two isomers: *cis,syn-* (left) and *cis,anti*-[(dmso)$_2$Pt(2-Tol)$_2$] (right, with full numbering; shown is only one of the two independent molecules). Shown are 30% thermal ellipsoids; H atoms are omitted for clarity.

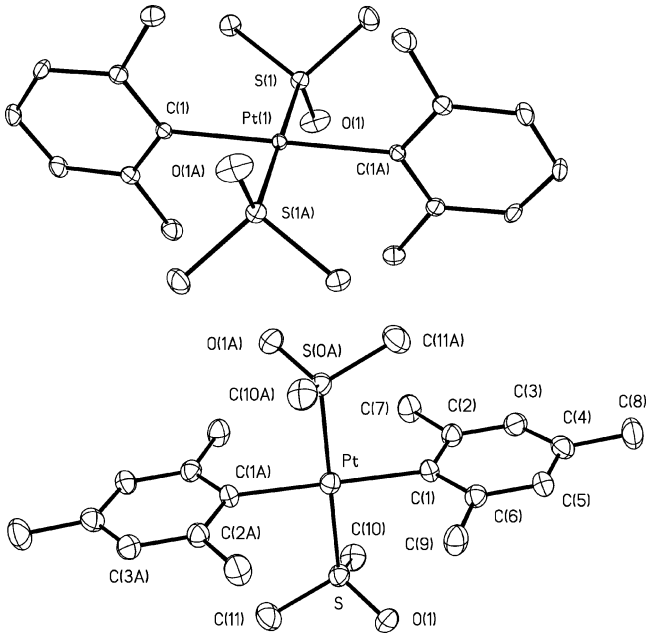

Figure 2. Molecular structures of *trans*-[(dmso)$_2$Pt(Xyl)$_2$] (above) and *trans*-[(dmso)$_2$Pt(Mes)$_2$] (293 K) (below, with numbering). Shown are 30% thermal ellipsoids; H atoms are omitted for clarity.

short O···H−CH$_2$−S contacts were found: d(H···O) = 2.294(19) Å; d(C···O) = 3.222(16) Å; angle O···H−C = 157.6(4)°. The values were not significant for effective H bridges; furthermore the methyl group is not a very good H-donor.[9] For the other compounds with the exception of the xylyl derivative similar O···H contacts were found that are even longer. Therefore no impact of these contacts on the molecular properties is expected.

The molecular structures confirm the conformations from spectroscopy in fluid solution: For the tolyl derivatives we found two *cis*-configured isomers which differ in the orientation of the methyl substituent relative to the binding plane (*syn* or *anti*) as shown in Figure 1. The xylyl and mesityl derivatives have a *trans* orientation of the two aryl groups (Figure 2); the platinum atom lies on a center of symmetry in both cases. All structures showed nearly perfect planar surrounding of the platinum center, as can be seen from the sum of angles and the small CCPt/SSPt tilt angles (Table 2).

It is interesting to note that for [(dmso)$_2$Pt(Mes)$_2$] a preliminary XRD experiment at 173(2) K (on a four-circle diffractometer) has led to a structure solution in the unusual C_2 space group, with a nonplanar structure (sum of angles: 405.9(2)°). In view of this very unusual pattern we re-examined the crystal using a CCD device, which finally led to the planar structure in $P2_1/c$. The 173(2) K dataset was then successfully solved using $P2_1/c$ as an input space group with essentially the same structure as found at 293(2) K. Details of the C_2 structure solution can be found in the Supporting Information.

The bond lengths and angles around the platinum atom in the series of complexes nicely reflect the *trans* influence.[10] For the *cis*-configured compounds the Pt−S distances were markedly longer due to the strong *trans* aryl ligand, and the Pt−C distances were consequently shorter. Lengthening of the Pt−S bond in the *cis* derivatives goes along with lengthening of the S−O bond, which can be explained by a higher degree of back-bonding from platinum to antibonding π^*(S═O) orbitals. The absolute values are both rather large compared to other structurally characterized dmso platinum complexes, in which the Pt−S bond length usually lies around 2.22 Å and the S−O bond around 1.46 Å or below, depending on the strength of the *trans*-oriented co-ligand.[11]

No difference is observed within the series of structures for the distances between platinum and the ortho methyl groups, which range from 3.28 to 3.42 Å. The tilt angles of the aryl ligands toward the coordination plane CCPtSS range from 70° to 90°. Since 90° would be the optimum for steric reasons, this is remarkable and no difference is observed between *cis* and *trans* conformers in that respect. We have noted this before for related *cis*-configured diimine platinum complexes (angles around 70°) and have ascribed this effect to an optimization of ligand-to-metal overlap in conjunction with metal-mediated ligand-to-ligand interaction.[12]

(9) Steiner, T. *Angew. Chem., Int. Ed.* **2002**, *41*, 48−78.

(10) Hartley, F. R. *The Chemistry of Platinum, Palladium*; John Wiley & Sons: New York, 1973.

(11) (a) Calligaris, M.; Carugo, O. *Coord. Chem. Rev.* **1996**, *153*, 83. (b) Priqueler, J. R. L.; Rochon, F. D. *Inorg. Chim. Acta* **2004**, *357*, 2167−2175. (c) Nédélec, N.; Rochon, F. D. *Inorg. Chem.* **2001**, *40*, 5236−5244. (d) Zucca, A.; Doppiu, A.; Cinellu, M. A.; Stoccoro, S.; Minghetti, G.; Manassero, M. *Organometallics* **2002**, *21*, 783−785.

(12) Klein, A.; van Slageren, J.; Záliš, S. *Eur. J. Inorg. Chem.* **2003**, 1917−1938.

Table 3. Experimental and ADF/BP-Calculated Structural Data for Complexes [(dmso)$_2$Pt(Ar)$_2$]

	exptl structure from single-crystal XRD	calcd bonding energy (kcal/mol)
[(dmso)$_2$Pt(Ph)$_2$]	*cis*[8] (293 K)	*cis:* −5663.4 *trans:* −5652.0
[(dmso)$_2$Pt(2-Tol)$_2$] (*anti*)	*cis,anti* (173 K)	*cis,anti*: −6414.6 *trans,anti*: −6404.1
[(dmso)$_2$Pt(2-Tol)$_2$] (*syn*)	*cis,syn* (293 K)	*cis,syn*: −6414.5 *trans,syn*: −6404.3
[(dmso)$_2$Pt(3-Tol)$_2$]	-	*cis,anti*: −6409.3 *trans,anti*: −6398.1
[(dmso)$_2$Pt(4-Tol)$_2$]	-	*cis*: −6408.9 *trans*: −6397.5
[(dmso)$_2$Pt(Xyl)$_2$]	*trans* (173 K)	*cis*: −7151.8 *trans*: −7153.7
[(dmso)$_2$Pt(Mes)$_2$]	*trans* (173 or 293 K)	*cis*: −7903.4 *trans*: −7908.0

ADF/BP-calculated bonding energies for each a *cis* and a *trans* conformer of selected examples (Ph, 2-Tol(*syn* and *anti*), 3-Tol(*anti*), Xyl and Mes) are listed in Table 3. The thus calculated ground state molecular structures agree fully with the found structures. Essentially no energy difference was obtained for the two stereoisomers (*syn* and *anti*) for the *cis*-2-Tol derivative, which is in agreement with their 1:2 occurrence in fluid solution.

NMR Spectroscopy and Calculations. The purified complexes were submitted to multiple (^{1}H, ^{13}C, and ^{195}Pt) NMR studies, essential data for structure determination from NMR data are summarized in Table 4, and full NMR data can be found in Tables 5−7 in the Experimental Section.

From the NMR data, in particular the ^3JPt−CH$_3$ and ^1JPt−C(1) coupling constants (Table 4), a clear-cut difference can be drawn between the phenyl derivative and complexes with monomethylated aryl ligands on one side and the 2,6-dimethyl and higher substituted derivatives on the other side. The ^3JPt−CH$_3$ coupling constants of the former are markedly smaller and ^1JPt−C(1) markedly larger than the values found for the higher substituted derivatives. Both findings are indicative of a shorter Pt−C bond, and thus the low-substituted derivatives are assigned to *cis* configurations whereas the higher substituted ones are *trans* configured. The calculations for both isomers within the whole series of complexes give a substantially larger ^1JPt−C(1) value in the case of the *cis* conformation. The calculated data are in agreement with the experimental trends and clearly support the assignment of *cis* and *trans* conformations. Excellent agreement of the calculation with spectroscopic data can be stated for the ^1JPt−C(1) coupling constant. Within the two series of the *cis*- and *trans*-configured compounds the ^1JPt−C(1) coupling constant reflects nicely the substitution pattern. The coupling constants are markedly increased for 2-Tol > 4-Tol compared to Ph. As expected for the impact of the meta position, the 3-Tol derivative exhibits a decreased coupling constant. A view of the complete

Table 4. Selected Experimental and Calculated NMR Data for Complexes [(dmso)$_2$Pt(Ar)$_2$]

	^3JPt−CH$_3$ dmso (Hz)	^1JPt−C(1) (Hz)	δ^{195}Pt (ppm)	conformation from NMR data	calcd ^1JPt−C(1) (Hz)
[(dmso)$_2$Pt(Ph)$_2$]	14.9	994.8	−4217	*cis*	*cis:* 1018.3 *trans*: 538.7
[(dmso)$_2$Pt(2-Tol)$_2$] (*anti*)	13.8, 15.5	1022.3	−4157	*cis*	*cis,anti:* 1042.9 *trans,anti*: 548.1
[(dmso)$_2$Pt(2-Tol)$_2$] (*syn*)	14.1, 16.0	1021.3	−4165	*cis*	*cis,syn:* 1029.2 *trans,syn*: 536.1
[(dmso)$_2$Pt(3-Tol)$_2$]	14.8	945.5	−4220	*cis*	*cis,anti:* 1017.3 *trans,anti*: 536.1
[(dmso)$_2$Pt(4-Tol)$_2$]	14.9	1002.6	−4212	*cis*	*cis:* 1027.5 *trans*: 541.3
[(dmso)$_2$Pt(Xyl)$_2$]	28.8	602.9	−4146	*trans*	*cis*: 1139.6 *trans*: 541.2
[(dmso)$_2$Pt(Mes)$_2$]	28.6	605.0	−4148	*trans*	*cis*: 1130.4 *trans*: 546.0
[(dmso)$_2$Pt(Me$_5$Ph)$_2$]	28.5	617.5	−4089	*trans*	-

Table 5. ^{1}H NMR Data of Complexes [(dmso)$_2$Pt(Ar)$_2$][a]

	δ (ppm) J_{H-Pt} (Hz)								
Ar	H$_2$	H$_6$	H$_3$	H$_5$	H$_4$	*o*-CH$_3$	*m*-CH$_3$	*p*-CH$_3$	CH$_3$-dmso
Ph	7.30 *69.7*	7.30 *69.7*	6.97	6.97	6.83				2.78 *14.94*
2-Tol (*anti*)		7.30 *77.8*	6.90	6.83	6.79	2.71 *6.7*			2.92, 2.59 *13.8, 15.5*
2-Tol (*syn*)		7.32 *73*	6.88	6.81	6.77	2.59 *6.2*			2.80, 2.76 *14.1, 16.0*
3-Tol	7.15 *70.9*	7.10 *68.8*		6.84 *26.8*	6.66		2.19		2.77 *14.84*
4-Tol	7.15 *69.3*	7.15 *69.3*	6.81	6.81				2.16	2.78 *14.9*
Xyl			6.93	6.93	6.93	2.67 *5.8*			2.72 *28.8*
Mes			6.78			2.61 *5.3*		2.21	2.71 *28.7*
Me$_5$Ph						2.73 *4.5*	2.17	2.18	2.69 *28.5*

[a] Chemical shifts in ppm and J_{H-Pt} in Hz, as measured in CD_2Cl_2.

Table 6. ^{13}C NMR Data of Complexes [(dmso)$_2$Pt(Ar)$_2$]^a

	δ (ppm) J_{C-Pt} (Hz)									
	C_1	C_2	C_6	C_3	C_5	C_4	*o*-CH_3	*m*-CH_3	*p*-CH_3	C_{dmso}
Ph	146.67	128.13	128.13	136.38	136.38	123.94				43.71
	994.8	*70.7*	*70.7*	*38.4*	*38.4*	*12.7*				*33.9*
2-Tol	145.99	129.35	125.10	142.61	136.52	123.89	26.11			43.41, 43.49
(*anti*)^b	*1022.3*	*55.0*	*75.7*	*27.4*	*41.6*	*10.2*	*70.1*			*36.6, 30.2*
2-Tol	145.76	128.91	125.09	142.32	135.89	123.92	27.41			43.51, 43.78
(*syn*)^b	*1021.3*	*55.0*	*75.7*	*26.5*	*29.6*	*10.2*	*79.5*			*33.7, 31.5*
3-Tol	146.50	137.40	127.85	133.26	137.02	124.71		21.52		43.58
	945.5	*76.4*	*79.3*	*49.9*	*48.8*	*14.2*				*33.3*
4-Tol	142.50	128.93	128.93	135.95	135.95	133.04			20.81	43.69
	1002.6	*78.3*	*78.3*	*40.8*	*40.8*	*14.8*				*33.5*
Xyl	158.37	127.18	127.18	145.51	145.51	124.84	24.80			45.10
	602.9	*24.6*	*24.6*	*4.4*	*4.4*	*< 2.8*	*28.9*			*78.8*
Mes	154.10	128.30	128.30	145.23	145.23	133.91	24.72		20.89	45.20
	605	*24.7*	*24.7*	*4.4*	*4.4*	*3.1*	*29.1*			*79.2*
Me_5Ph	154.23	132.54	132.54	140.15	140.15	130.95	23.42	16.80	16.51	45.40
	617.5	*24.2*	*24.2*	*4.5*	*4.5*	*< 1*	*28.7*	*5.3*	*3.1*	*79.3*

^{a} Chemical shifts in ppm and J_{C-Pt} in Hz, as measured in CD_2Cl_2. ^{b} Measured in $CDCl_3$.

Table 7. ^{195}Pt NMR Data of Complexes [(dmso)$_2$Pt(Ar)$_2$]^a

Ar	δ^{195}Pt (ppm)
Ph	−4217
2-Tol (*anti*)	−4157
2-Tol (*syn*)	−4165
3-Tol	−4220
4-Tol	−4212
Xyl	−4146
Mes	−4148
Me_5Ph	−4089

^{a} Chemical shifts in ppm as measured in $CDCl_3$.

NMR data in Tables 5 and 6 shows that also all other values nicely follow these trends.

It is furthermore interesting to note that the pentafluorophenyl derivative [(dmso)$_2$Pt(C_6F_5)$_2$] has been shown to occur exclusively in the *cis* conformation.[13] The ^3JPt−CH_3 coupling of 18 Hz is markedly enhanced within the series of *cis*-configured complexes, showing the electron-withdrawing effect of fluorine substitution, which obviously strengthens the Pt−S bond.

For the 2-tolyl derivative two sets of signals (2:1 ratio) were always found, both clearly indicating the presence of complexes with *cis* configuration. Detailed analysis of the results of phase-sensitive ^{1}H gs-NOESY NMR experiments enabled us to assign them to the *syn* and *anti* isomers which arise from the asymmetry of the tolyl substituent.[2,14,15] The key to this stereochemical assignment was the observation that the major isomer showed a strong NOE correlation signal with negative intensity between the H-6 proton and the *o*-CH_3 group, while this correlation was absent for the minor isomer (Figure 3). If this cross signal would arise from dipolar interaction between the aromatic and methyl protons in the *same* substituent, it would be visible for both isomers, as the mean H−H distance (under consideration of a freely rotating CH_3 group) within the rigid tolyl framework is essentially identical in both cases. The absence of a visible cross-peak for just one isomer proves thus that (a) the NOE correlation must result from interaction of the H-6 and *o*-CH_3 protons in two different substituents and (b) the major isomer is the one with the shorter H−H distance. This species was thus assigned as the *anti* isomer, where the H-6 and *o*-CH_3 protons in different substituents lie on the same side with respect to the metal coordination plane and are separated by a shorter distance than in the *syn* isomer.

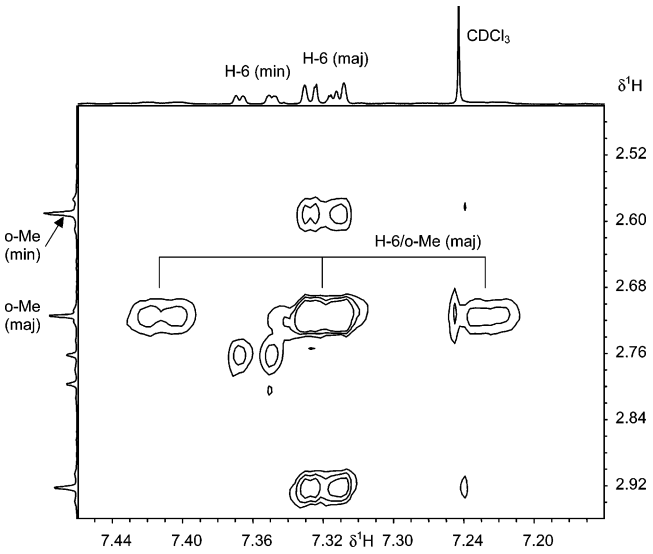

Figure 3. Expansion of a phase-sensitive two-dimensional ^{1}H gs-NOESY spectrum (mixing time 750 ms) of *cis*-[(dmso)$_2$Pt(2-Tol)$_2$] showing correlations between the aromatic H-6 protons with the protons in *o*-CH_3 and CH_3-dmso substituents (only negative contour levels shown). The projections are expansions of a normal ^{1}H NMR spectrum. The signals of the H-6 and *o*-CH_3 protons in both isomers and the three components of the correlation signal (referring to the parent resonance and ^{195}Pt satellites) are labeled appropriately.

Further analysis of the NOESY spectra showed *inter*molecular cross-peaks connecting the two diastereotopic CH_3-dmso and the *o*-CH_3 signals of both isomers with each other and also the CH_3-dmso signals of both isomers with the resonance of free dmso which was present in the sample in small concentration (Figure 4). Because of their positive phase, we interpret these signals as arising from chemical exchange rather than NOE (this assignment is corroborated by the observation of a small NOE correlation with negative intensity

(13) Cullinane, C.; Deacon, G. B.; Drago, P. R.; Hambley, T. W.; Nelson, K. T.; Webster, L. K. *J. Inorg. Biochem.* **2002**, *89*, 293−301.
(14) Biagini, M. C.; Ferrari, M.; Lanfranchi, M.; Marchio, L.; Pellinghelli, M. A. *J. Chem. Soc., Dalton Trans.* **1999**, 1575−1580.
(15) Plutino, M. R.; Scolaro, M. L.; Albinati, A.; Romeo, R. *J. Am. Chem. Soc.* **2004**, *126*, 6470−6484.

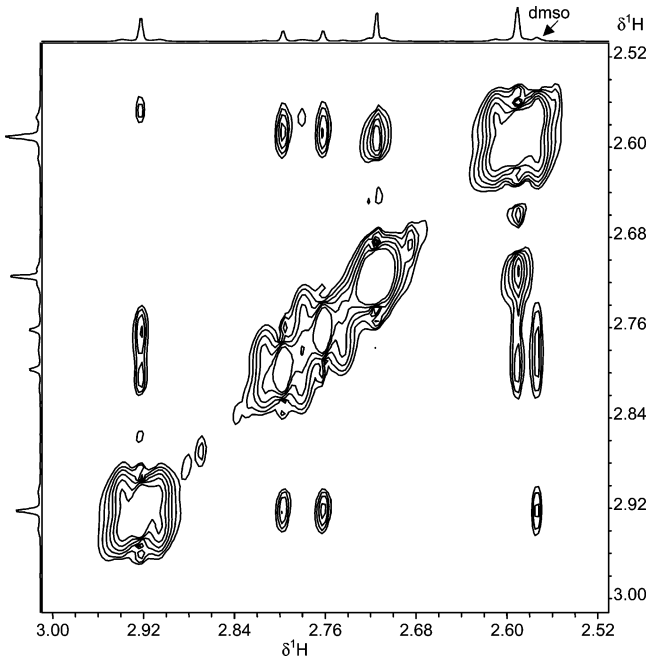

Figure 4. Expansion of a phase-sensitive two-dimensional ^{1}H gs-NOESY spectrum (mixing time 750 ms) of *cis*-[(dmso)$_2$Pt(2-Tol)$_2$] showing correlations between the protons in *o*-CH_3 and diastereotopic CH_3-dmso substituents with each other (only positive contour levels shown). The signal at highest field is assigned to a superposition of one of the CH_3-dmso signals of the major isomer and the *o*-CH_3 signal of the minor isomer; the singlet arising from a small amount of free dmso overlapping with one of the ^{195}Pt satellites of this signal is labeled.

between the signals of the two diastereotopic dmso-methyl groups in the *anti* isomer). A rationalization of these peaks can be given by assuming dynamic isomerization between both isomers; the involvement of free dmso suggests that this process follows presumably a dissociative mechanism.[5,15] A quantitative analysis of cross-peak intensities, which might in principle provide information on the relative rates of dmso exchange and interconversion of *syn* and *anti* isomers by rotation, was prevented by incomplete resolution of closely spaced or accidentally superimposed correlation signals. It should be noted that the expected cross-peaks connecting the aromatic protons could not be detected, presumably as a consequence of severe signal overlap and much lower signal intensities.

Experimental Section

NMR Experiments. ^{1}H NMR spectra for analytical purposes were recorded on a Bruker AC250 spectrometer. Further ^{1}H, ^{13}C{^{1}H}, and ^{195}Pt{^{1}H} NMR spectra were recorded on a Bruker DPX-300 NMR spectrometer operating at 300, 75.47, and 64.52 MHz, respectively. Chemical shifts are relative to the internal chloroform peak at δ 7.26 for ^{1}H and δ 77.0 for ^{13}C and $Na_2[PtCl_6]$ in D_2O for ^{195}Pt. A 90° pulse was used in every case. Two-dimensional NMR measurements for the assignment of the ^{1}H, ^{13}C, and ^{195}Pt signals of the *syn* and *anti* conformers of [(dmso)$_2$Pt(2-Tol)$_2$] were carried out using a Bruker Avance 400 spectrometer (^{1}H: 400.13 MHz, ^{195}Pt: 86.01 MHz, ^{13}C: 100.3 MHz) in $CDCl_3$ at 30 °C; chemical shifts were referenced to external TMS (^{1}H, ^{13}C) or K_2PtCl_6 (Ξ = 21.496784 MHz, ^{195}Pt). The assignment of ^{13}C and ^{195}Pt resonances was obtained from gradient selected (gs) ^{1}H,^{13}C HMQC and HMBC and ^{1}H,^{195}Pt HMQC spectra. Conformational assignments and the analysis of dynamic properties were derived from two-dimensional ^{1}H gs-NOESY NMR spectra using mixing times between 500 and 750 ms. All 2D NMR spectra were recorded by using standard pulse sequences from the Bruker pulse program library.

Crystal Structures. For the complexes *cis,anti*-[(dmso)$_2$Pt-(2-Tol)$_2$], *trans*-[(dmso)$_2$Pt(Xyl)$_2$], and *trans*-[(dmso)$_2$Pt(Mes)$_2$] data collection was performed at T = 173(2) K on a Siemens P4 diffractometer with Mo Kα radiation (λ = 0.71073 Å) employing $\omega-2\theta$ scan technique. The data for *cis,syn*-[(dmso)$_2$Pt-(2-Tol)$_2$] and again for *trans*-[(dmso)$_2$Pt(Mes)$_2$] were collected at T = 293(2) K on a KappaCCD device (Mo Kα: λ = 0.71073 Å; horizontally mounted graphite crystal; 95 mm CCD camera on κ-goniostat) using Collect (Nonius BV, 1997−2000) software. All structures were solved by direct methods using the SHELXTL package,[16] and refinement was carried out with SHELXL97 employing full-matrix least-squares methods on F^2 [17] with $F_o^2 \geq 2\sigma(F_o^2)$ with the results shown in Table 2 (or Supporting Information). All non-hydrogen atoms were treated anisotropically; hydrogen atoms were included by using appropriate riding models.

CCDC-262651 for *cis,syn*-[(dmso)$_2$Pt(2-Tol)$_2$], -262652 for *cis,anti*-[(dmso)$_2$Pt(2-Tol)$_2$], -262653 for *trans*-[(dmso)$_2$Pt(Xyl)$_2$], and -262654 for *trans*-[(dmso)$_2$Pt(Mes)$_2$] contain the full crystallographic data for this paper. These data can be obtained free of charge at www.ccdc.cam.ac.uk/conts/retrieving.html or from the Cambridge Crystallographic Data Centre, 12 Union Road, Cambridge, CB2 1EZ UK. Fax: + 44-1223-336−033; e-mail: deposit@ccdc.cam.ac.uk.

Quantum Chemical Calculations. Ground state electronic structure calculations have been done on the basis of density-functional theory (DFT) methods using ADF2004.01.[18] Nuclear spin−spin coupling constants were calculated by the CPL module[19] within ADF2004.01.

Slater type orbital (STO) basis sets of triple-ζ quality with polarization functions were employed for geometry optimization. The inner shells were represented by the frozen core approximation (1s for C, O, 2p for S, and 1s−4d for Pt were kept frozen). Core electrons were included for calculations of NMR parameters; here quadruple-ζ basis with four polarization functions was used for Pt. The following density functionals were used within ADF: the local density approximation (LDA) with VWN parametrization of electron gas data or the functional including Becke's gradient correction[20] to the local exchange expression in conjunction with Perdew's gradient correction[21] to the LDA expression (ADF/BP). The scalar relativistic (SR) zero-order regular approximation (ZORA) was used within this study.

Preparations. All manipulations were carried out under an atmosphere of argon. Solvents were dried and distilled prior to use. The stannanes (aryl)$SnMe_3$ were prepared according to literature procedures.[22]

Preparation of the Complexes [(dmso)$_2$PtAr$_2$] (Ar = 2-Tol, 3-Tol, 4-Tol, Xyl, Mes, Ph(Me)$_5$). In a typical reaction 6 mmol of Me_3SnAr (Ar = 2-Tol, 3-Tol, 4-Tol, Xyl, Mes, Ph-(Me)$_5$) dissolved in 20 mL of dimethyl sulfoxide was added to 500 mg (1.184 mmol) of [(dmso)$_2$PtCl$_2$], and the mixture was

(16) Sheldrick, G. M. *SHELXTL*; Bruker Analytical X-Ray Systems: Madison, WI, 1998.
(17) Sheldrick, G. M. *SHELXL-97: A program for Crystal Structure Determination*; Universität Göttingen: Göttingen, Germany, 1997.
(18) (a) te Velde, G.; Bickelhaupt, F. M.; van Gisbergen, S. J. A.; Fonseca Guerra, C.; Baerends, E. J.; Snijders, J. G.; Ziegler, T. *J. Comput. Chem.* **2001**, *22*, 931−967. (b) *ADF2004.01, SCM*; Theoretical Chemistry, Vrije Universiteit: Amsterdam, The Netherlands, http://www.scm.com.
(19) (a) Autschbach, J.; Ziegler, T. *J. Chem. Phys.* **2000**, *113*, 936−947. (b) Autschbach, J. A.; Ziegler, T. *J. Chem. Phys.* **2000**, *113*, 9410−9418.
(20) Becke, A. D. *Phys. Rev. A* **1988**, *38*, 3098−3100.
(21) Perdew, J. P. *Phys. Rev. A* **1986**, *33*, 8822−8824.
(22) Eaborn, C.; Hornfeld, H. L.; Walton, D. R. M. *J. Organomet. Chem.* **1967**, *10*, 529−530.

stirred at 90−100 °C for 8 h. The solvent and $ClSnMe_3$ were distilled off under reduced pressure. The resulting colorless precipitate was washed with pentane and dried in vacuo. Recrystallization of the product from CH_2Cl_2 gave off-white crystals.

Preparation of [(dmso)$_2$PtPh$_2$]. To a stirred dimethyl sulfoxide (20 cm^3) solution of 500 mg (1.205 mmol) of K_2PtCl_4 was added 1.452 g (6.025 mmol) of $PhSnMe_3$. After stirring the mixture at 70 °C for 8 h, the solvent and $ClSnMe_3$ were distilled off under reduced pressure. The resulting precipitate was dissolved in CH_2Cl_2, and residual KCl was filtered off through a G-3 glass filter. After evaporation of the solvent 555 mg (1.098 mmol, 91.1%) of the colorless product [(dmso)$_2$PtPh$_2$] was obtained.

Acknowledgment. This work was supported by the Deutsche Forschungsgemeinschaft, Fonds der Chemischen Industrie, and the European Community (program COST D14/D35). S.Z. also acknowledges financial support by the Grant Agency of the Academy of Sciences of the Czech Republic (grant 1ET400400413). Further support for this work came from the BMBF (Project No. IND 99/060−Indo-German bilateral program) as well as from Johnson Matthey PLC ("JM") for a loan of K_2PtCl_4.

Supporting Information Available: Further tables with full structural data are available for the two structure solutions for [(dmso)$_2$Pt(Mes)$_2$] (nonplanar C_2 at 173 K and planar $P2_1/c$ at 293 K). Figures showing the crystal structures (unit cell) of all complexes and an expansion of a phase-sensitive two-dimensional ^{1}H gs-NOESY spectrum (mixing time 750 ms) of *cis*-[(dmso)$_2$Pt(2-Tol)$_2$] showing correlations between the protons in *o*-CH_3 and CH_3-dmso substituents with each other (only positive contour levels shown) are also available free of charge via the Internet at http://pubs.acs.org.

OM050076+